JPP Journal of Pharmacy and Pharmacology

JPP 2007, Supplement 1: A1–A6

SHORT TALKS

New Scientist Session "Recent advances in pharmaceutical science"

1
The formation of nano-complexes between insulin and self-assemblies based on novel amphiphilic graft polymers: the effect of polymer architecture on the complexation efficiency

C. J. Thompson and W. P. Cheng

Robert Gordon University, School of Pharmacy, Schoolhill, Aberdeen, AB10 1FR, UK.
E-mail: c.thompson@rgu.ac.uk

Objectives To determine the effect of amphiphilic graft polymer architecture (level of hydrophobic substitution and addition of hydrophilic moieties) on the complexation efficiency of the self-assemblies with insulin. Traditional technologies, such as co-administration of protease inhibitors and encapsulation within solid nanoparticles, have been used to deliver proteins and peptides orally (Simon et al 2006). Recently a new approach utilising self-assembled polymers to form nano-complexes with insulin has been employed. It was reported that these delivery systems potentially protect insulin from gastrointestinal degradation and increase the oral bioavailability (Simon et al 2006). We have successfully synthesised novel cationic amphiphilic graft polymers based on polyallylamine (PAA) and the ability of these polymers in forming nano-complexes with insulin was investigated.

Methods Novel amphiphilic graft polymers were synthesised by grafting PAA with differing amounts (x & y %mole) of aliphatic moieties (Am) and subsequently quaternised (Q) with a quaternisation reagent. The polymer and insulin solutions were made up in Tris buffer (pH 7.4) and a fixed insulin concentration (0.3 mg mL^{-1}) was used. Complexation was carried out at polymer: insulin mass ratios of 2:1, 1:1 and 1:3. Complexes were left at 20 °C for 2 h before particle size, zeta potential (Zetasizer Nano-ZS, Malvern Instruments, UK) and complexation efficiency (Luminescence spectrometer LS55, Perkin Elmer, UK) were determined. The concentration of insulin in the nano-complexes was calculated from a calibration graph (0.05–0.3 mg mL^{-1}, $R^2 = 0.98$).

Table 1 Physical properties and complexation efficiency (CE) (%) of insulin complexes (n = 3)

Polymer insulin: mass ratio	CE (%)	Size (nm)	Zeta potential (mV)
Am_x			
1:3	94 (1)	190 (117)	34.2 (1.3)
1:1	84 (2)	144 (4)	35.4 (1.0)
2:1	81 (2)	162 (2)	35.8 (3.0)
Am_y			
1:3	88 (4)	90 (2)	36.2 (2.0)
1:1	76 (2)	146 (1)	35.7 (1.0)
2:1	69 (3)	162 (2)	36.7 (2.6)
QAm_x			
1:3	89 (3)	479 (202)	31.9 (1.4)
1:1	95 (4)	288 (106)	33.6 (1.3)
2:1	103 (1)	108 (1)	33.2 (1.9)
QAm_y			
1:3	89 (1)	5810 (1480)	17.9 (0.4)
1:1	91 (5)	344 (199)	34.6 (1.6)
2:1	97 (1)	120 (2)	30.3 (2.9)

±s.d. given in parentheses.

Results Insulin is negatively charged at pH 7.4 and since all formulations have positive zeta potentials, this indicates the complexation was successful with CE up to 103% for QAm_x (Table 1). From the data it appears that non-quaternised and quaternised polymers exhibit different trends. Higher levels of complexation were achieved at lower non-quaternised polymer concentrations. However, CE increased when higher concentrations of quaternised polymer were used, possibly due to an increased level of positive charge of polymers forming compact nano-complexes with insulin.

Conclusions These novel amphiphilic polymers are able to form nano-complexes with insulin and will be subjected to further *in vitro* and *in vivo* testing to determine their suitability as insulin delivery systems.

Simon, M., et al (2006) *Eur. J. Pharm. Biopharm*. In press

2
Application of interpolymer complexation via hydrogen-bonding to develop nanoparticles, mucoadhesive films and tablets

V. V. Khutoryanskiy and O. V. Khutoryanskaya

University of Reading, School of Pharmacy, Whiteknights, Reading, RG6 6AD, UK.
E-mail: v.khutoryanskiy@reading.ac.uk

Objectives To develop nanoparticles and mucoadhesive films based on interpolymer complexes (IPC) and blends of poly(acrylic acid) and methylcellulose.

Methods The complexation between poly(acrylic acid) (PAA) and methylcellulose (MC) in aqueous solutions, as well as the structure and stability of nanoparticles, were studied by turbidimetric titration, isothermal titration calorimetry, dynamic light scattering and transmission electron microscopy. The mucosal compatibility of the films was estimated by using the Slug Mucosal Irritation Test (Adriaens & Remon 1999).

Results Hydrophobic IPC are formed by mixing 0.2 wt % solutions of PAA and MC at pH < 3.5. These complexes exist as stable spherical nanoparticles in the mixtures containing 30 wt % of MC and 70 wt % of PAA (Figure 1). The size of these nanoparticles varies within 15–550 nm depending on solution pH (pH 1.0–3.2) and aging time. These nanoparticles can be promising for formulation of poorly soluble drugs (Khutoryanskiy 2007). The complexes formed at other polymer ratios tend to aggregate and precipitate quickly. The IPC precipitates were washed with distilled water and freeze-dried. The material obtained was used to prepare mucoadhesive tablets. The films were prepared by casting aqueous mixtures of PAA-MC at different ratios and pH. The miscibility of the polymers in the blends was analysed by scanning electron microscopy. It was found that the films cast at 3.0 < pH < 6.0 were transparent and had homogeneous morphology, which miscibility is ensured by weak hydrogen bonding between the polymers. At pH < 3.0 the films were not uniform because of precipitation of IPCs and at pH > 6.0 the polymers formed immiscible blends. Mucosal compatibility of the films is improved with increase in MC content in the blends.

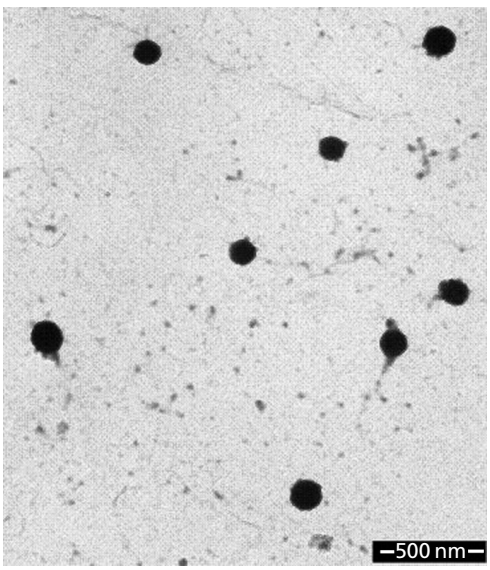

Figure 1 PAA-MC (70:30 wt %) nanoparticles at pH 2.59.

Conclusions Interpolymer complexation between PAA and MC offers a simple and inexpensive method to prepare nanoparticles, mucoadhesive films and tablets.

Acknowledgements This work was financially supported by the BBSRC (BB/E003370/1) and the Royal Society (Research grant 2006/R1).

Adriaens & Remon (1999) *Pharm. Res*. **16**: 1240–1244
Khutoryanskiy, V. V. (2007) *Int. J. Pharm*. **334**: 15–26

3
Dynamic contrast enhanced, magnetic resonance imaging (DCE-MRI) as a predictor of drug and nanomedicine transport in solid tumour models

S. MacLellan[1,2], I. F. Uchegbu[2], W. Holmes[3], B. Condon[4] and A. G. Schätzlein[2]

[1]University of Strathclyde, Medical Devices Doctoral Training Centre, Bioengineering Unit, Glasgow, G4 0NW, [2]The School of Pharmacy, University of London, London, WC1N 1AX, [3]University of Glasgow, 7T MR Facility, Wellcome Surgical Institute, Glasgow, G61 1QH and [4]University of Glasgow, Department of Clinical Physics, Southern General Hospital, Glasgow, G51 4TF, UK.
E-mail: steven.maclellan@pharmacy.ac.uk

Objectives To use high-resolution 4D multimode MRI to analyse transport processes in tumours. Tumours that can not be treated by surgery or radiotherapy are normally treated by the intravenous injection of anti-cancer drugs and these agents then have to travel through the blood and extravasate to reach the cancer cells. Tumours develop barriers to the transport of both low molecular weight cytotoxics and nanomedicines (Cassidy & Schätzlein 2004). MRI enables tumour transport of low molecular weight drugs and particulates to be studied.

Methods A polymeric contrast agent (Polymer-DTPA-Gd) was synthesised by conjugating polymer fragments (10 kDa) with the chelating agent diethylene-triamine-pentaacetic-acid (DTPA) and incubating with the paramagnetic ion gadolinium (Gd). This compound was characterised for conjugate composition and gadolinium content using elemental analysis, ^{1}H NMR, inductively coupled plasma atomic emission and an arsenazo based colorimetric assay. Mice bearing either A431 or B16F10 tumours were injected intravenously with a low molecular weight contrast agent (DTPA-Gd) or Polymer-DTPA-Gd and the entire tumour volume imaged in true 3D using a FLASH sequence and the vasculature was imaged using magnetic resonance angiography (MRA). This is the first report of scanning to a resolution of 1 mm^3 achieved using a Bruker BioSpin 7T system and a custom designed surface coil. The raw scanning data was handled using IDL (Research Systems, USA).

Results The polymeric agent proved useful in visualising the tumour vasculature (Figure 1) and also highlighted the molecular weight dependence of drug transport within tumours. Transport maps, constructed from 3D scans, show contrast agent movement radially inwards from the tumour rim towards the tumour centre consistent with blood supply.

Conclusions MRI allows the multimodal, dynamic and functional characterisation of tumour barriers, nanomedicine transport, and therapeutic response with the parameters being directly comparable with clinical MRI data. These techniques help correlate our understanding of animal nanomedicine pharmacology with the human disease and thus may ultimately support the clinical development of these therapies.

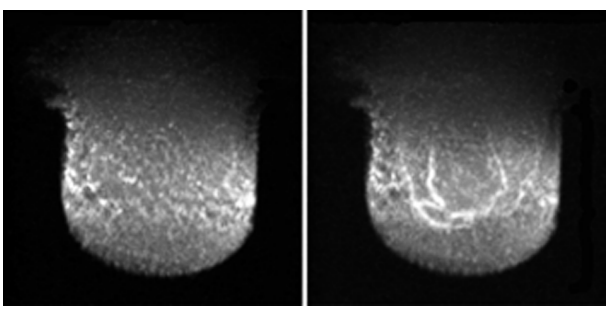

Figure 1 Coronal maximum intensity projection images of an A431 xenograft obtained before (left) and after (right) the intravenous injection of Polymer-DTPA-Gd.

Cassidy, J., Schätzlein, A. G. (2004) *Expert Rev. Mol. Med*. **6**: 1–17

4
Microspheres for the delivery of TB sub-unit vaccines: entrapped or adsorbed antigen?

D. J. Kirby, V. W. Bramwell and Y. Perrie

Aston University, Aston Triangle, Birmingham, B4 7ET, UK.
E-mail: kirbydj@aston.ac.uk

Objectives To investigate the effect of formulation type, and hence the way in which antigen is associated, on the physico-chemical characteristics and immunological efficacy of microspheres for the delivery of the sub-unit tuberculosis (TB) vaccine antigen, Ag85B-ESAT-6.

Methods Poly(DL-lactide-co-glycolide) (PLGA) (75:25) microspheres incorporating dimethyl dioctadecylammonium (DDA) were prepared by either: (1) the double emulsion solvent evaporation method (w/o/w), with Ag85B-ESAT-6 entrapped within the internal aqueous phase; or (2) the single emulsion solvent evaporation method (o/w), with Ag85B-ESAT-6 adsorbed to the surface. In both cases, 0.75% (w/v) Chitosan (low molecular weight) was used as the external aqueous phase. BALB/c mice then received the microsphere formulations intramuscularly, with each mouse receiving three doses at intervals of two weeks. Serum samples were taken at 12 days after the first administration and at two-week intervals thereafter and analysed for the presence of anti-Ag85B-ESAT-6 IgG1, IgG2a and IgG antibodies by enzyme-linked immunosorbent assay (ELISA). Upon termination, spleens were removed and used to assess antigen specific proliferative responses and cytokine production. Experimentation adhered to the 1986 Scientific Procedures Act (UK), with all protocols subjected to ethical review and carried out in a designated establishment.

Results Both the o/w and the w/o/w formulation method produced microspheres within the desired sub-10 μm range (6.9 ± 0.4 μm and 3.0 ± 0.1 μm, respectively), whilst exhibiting a cationic surface charge (34.2 ± 2.3 mV and 39.1 ± 1.6 mV, respectively). However, the w/o/w formulation method yielded an Ag85B-ESAT-6 entrapment efficiency of just $24.2 \pm 4.2\%$, whereas the o/w formulation method exhibited a significantly higher Ag85B-ESAT-6 adsorption efficiency of $77.4 \pm 6.5\%$ ($P < 0.001$, t-test). The location of the antigen clearly has an influence on the type and level of antibody response achieved, with the o/w formulation (antigen adsorbed) showing increased levels of all antibodies investigated as compared to the w/o/w formulation (antigen entrapped), particularly at later time points. In addition, the o/w formulation shows a mixed antibody response, with both Th1 (IgG2a) and Th2 (IgG1) type antibodies showing significantly increased levels as compared to the naïve control ($P < 0.05$, Kruskal-Wallis followed by Dunn's post test). Nevertheless, the w/o/w formulation produced significantly higher cell proliferation than the o/w formulation ($P < 0.01$, Kruskal-Wallis followed by Dunn's post test), as well as enhanced levels of cytokine production, particularly for the Th1 type indicators gamma interferon (IFN-γ) and interleukin-2 (IL-2). These results suggest a greater emphasis on a cell-mediated immune response as compared to the o/w formulation, a desired facet for delivery systems targeting the treatment of disease such as TB.

Conclusions Microspheres prepared by the single oil-in-water emulsion technique (surface bound antigen) elicited enhanced antibody production as compared to their w/o/w counterparts, whereas the reverse was true for both antigen specific spleen cell proliferation and cytokine production. This apparent difference in immune response may be attributable to several factors, including size and zeta potential, although the most probable cause is the way in which the antigen is released and presented to the cells of the immune system.

5
Synthesis and topoisomerase II activity of halogenated cryptolepine analogues

P. Jerrum[1], C. W. Wright[2], A. Jewell[3], J. E. Brown[1] and S. Carrington[1]

[1]Kingston University, School of Pharmacy and Chemistry, Kingston University, Penrhyn Road, Kingston upon Thames, Surrey, KT1 2EE, [2]University of Bradford, School of Pharmacy, University of Bradford, Richmond Road, Bradford, West Yorkshire BD7 1DP and [3]Kingston University, Faculty of Health and Social Care Sciences, Penrhyn Road, Kingston upon Thames, Surrey, KT1 2EE, UK. E-mail: s.carrington@kingston.ac.uk

Objectives Cryptolepine is a tetracyclic aromatic natural product, isolated from West African shrubs of the *Cryptolepis* species, consisting of fused indol and quinoline rings. Due to its polyaromatic character it is able to intercalate into DNA, between base pairs and perpendicular to the axis of the double helix. Cryptolepine and its analogues have been investigated for their antimalarial and anti-cancer activity. The latter is our area of interest and has been related to intercalating ability and subsequent inhibition of topisomerase II. This enzyme is able to catalyse changes in DNA topology, through transient breaks and rejoining of double-stranded DNA. Due to topoisomerases being essential cellular enzymes within the cell cycle, they are key clinical targets for anti-cancer drugs. In this study we have synthesised

novel halogenated cryptoleines and have investigated their in vitro ability to inhibit topoisimerase II.

Methods Target compounds were synthesised using modifications of the methodologies from Rádl et al (2000) and Takeuchi et al (1992). 2-Aminobenzonitrile, or an analogue, was reacted with ethyl chloroformate followed by addition of 2-bromo-2′nitroacetophenone to produce a corresponding indol derivative. Cyclisation, brought about by sodium hydride, yielded quindolone derivatives, which were brominated in a phosphorous tribromide/phosphorous oxybromide mix. These bromoqundolines were methylated with methyl triflate in toluene to give 11-bromocryptolepines or simultaneous methylation and halogen exchange was brought about by methyl iodide in sulfolane, to give 11-iodocryptolepines. Topoisomerase II activity was assessed by use of a Topogen kit and agarose gel electrophoresis. DNA containing mini- and maxi-circles is linearised by topoisomerase II which, unlike the catenated maxicircles, can then migrate during electrophoresis. Introduction of sufficient concentration of an inhibitor prevents this linearization hence the corresponding band does not appear in the gel.

Results Table 1 shows the minimum inhibitory concentrations (MIC) of the cryptolepines synthesised. Halogenated analogues have previously been shown to have better cyctoxic activity than the parent compound (Wright et al 2001) and this is supported by all of the compounds showing comparable or better inhibitory activity than cryptolepine. Despite the large size of the iodine atom, which may be predicted to have an adverse effect on intercalation and hence topoisomerase II inhibition, these compounds show favourable activity in comparison to the smaller bromocryptolepine analogues.

Conclusions The halogenated cryptolepine analogues which we have studied show inhibition of topoisomerase II at concentrations between 10 and 0.1 μM. These compounds show equal or better activity in both their cytotoxicity and their topoisomerase activity compared with cryptolepine itself which suggests the two properties may have some connection.

Table 1 Topoisomerase II activities of the synthesised cryptolepine analogues

Cryptolepine analogue	MIC (μM)
Cryptolepine	10
11-Bromo	1.0
11-Iodo	0.5
9-Chloro-11-bromo	10
9-Chloro-11-iodo	1.0
8-Chloro-11-iodo	10

Rádl, S. (1999) *J. Heterocyclic Chem.* **37**: 855–862
Takeuchi, Y., et al (1992) *Chem. Pharm. Bull.* **40**: 1481–1485
Wright, C. W., et al (2001) *J. Med. Chem.* **44**: 3187–3194

6
Chitosan enriched proliposomes for pulmonary delivery of amphotericin B

S. Somavarapu[1], Y. Y. Albasaram[1], S. Loi[1], A. M. A. Elhissi[2], P. Stapleton[1] and K. Taylor[1]

[1]The School of Pharmacy, University of London, 29/39 Brunswick Square, Bloombsbury, London, WC1N 1AX and [2]The School of Pharmacy and Pharmaceutical Sciences, The University of Central Lancashire, Preston PR1 2HE, UK. E-mail: soma@pharmacy.ac.uk

Objectives Delivery of the antifungal agent amphotericin B (AmB) via aerosol inhalation may enhance its therapeutic effect and decrease toxicity in the treatment of pulmonary fungal infections (Shah & Misra 2004). The objective of the present work was to investigate the antifungal activity of chitosan enriched liposomes produced from AmB proliposomes.

Methods Liposomes were produced from ethanol-dimethyl sulfoxide-based soya phosphatidylcholine proliposome formulations by addition of isotonic sodium chloride or 0.1%w/v chitosan glutamate solutions. Drug:lipid ratio was 1:100. Liposomes were probe sonicated and filtered through 0.22 μm filters. Liposomal size (Z_{ave}) and surface charge (zeta potential) were determined using a Malvern ZetaSizer, and encapsulated AmB was measured using UV spectroscopy. The antifungal activity of the formulations was assessed against *Candidia albicans* ATCC 10231 by microdilution susceptibility testing in 96-well microtitre plates. Liposomes (2.5 mL) were placed in a Pari LC Star nebuliser attached to a TurboBoy N compressor and nebulisation undertaken to "dryness" into a twin impinger (TI). Aerosol output was determined gravimetrically, whilst drug output and deposition in the fine particle fraction (FPF) (i.e. lower stage of the TI) were estimated by UV analysis. The volume median diameter (VMD) of the aerosol droplets was determined using a Malvern 2600c laser diffraction analyser.

Results The surface charge of liposomes produced in the presence of chitosan showed positive values indicating the existence of chitosan on the surface of liposomes. Inclusion of chitosan had a minor effect on the mean liposome size whilst chitosan coating markedly enhanced AmB loading following hydration (Table1). Chitosan free liposomes loaded with AmB had activity against *C. albicians* similar to Fungizone (AmB desoxycholate) with MIC values of 0.25 and 0.5 μg/mL, respectively. The antifungal activity of AmB was enhanced four-fold with chitosan enriched liposomes (MIC value: 0.12 μg/mL). The VMD of the nebulised droplets was unaffected by the formulation, while aerosol output decreased when chitosan was included (Table 1), possibly due to increased fluid viscosity. Moreover, the FPF of AmB was approximately 90% for all reconstituted proliposome formulations.

Conclusions This study demonstrates that AmB can be efficiently incorporated into lipsomes produced by hydrating proliposomes with chitosan solutions. Chitosan coating of liposomes enhanced *in vitro* antifungal activity of amphotericin B, and the resultant formulations were efficiently delivered from a medical nebuliser.

Table 1 Size, surface charge, drug loading and aerosol properties of e liposome formulations

Formulation	Liposome size (nm) (PI)	Zeta potential (mV ± SD)	AmB Loading (%)	Aerosol output (%)	Aerosol VMD (μm)
PC	206.8 (0.210)	−3.6 ± 0.4	57.50	90.82	3.09 ± 0.11
PC-Chitosan glumate-113	230.0 (0.401)	+2.3 ± 0.3	71.25	81.75	3.06 ± 0.02
PC-Chitosan glumate-213	287.9 (0.452)	+2.8 ± 0.6	78.75	76.55	2.98 ± 0.14

Shah, S. P., Misra, A. (2004) *Drug Deliv.* **11**: 247–253